New magnetic data of the southern East China Sea and some geological interpretations

LUNING SHANG[1,2,3,4], XUNHUA ZHANG[2,3]*, RUNLIN DU[3], YONGGANG JIA[1,4], ZHENXING TIAN[2,3], BO HAN[2,3] AND CHUANSHENG YANG[2,3]

1 College of Environmental Science and Engineering, Ocean University of China, Qingdao 266100, P.R. China

2 Function Laboratory for Marine Mineral Resource Geology and Exploration, Qingdao National Oceanography Laboratory, Qingdao 266000, P.R. China

3 Institute of Marine Geology, Ministry of Land and Resources, Qingdao 266071, P.R. China

4 Key Laboratory of Marine Environment and Ecology, Ministry of Education, Qingdao 266100, P.R. China

* Corresponding author (xunhuazh@vip.sina.com)

Received: July 7, 2015; Revised: December 6, 2015; Accepted: March 4, 2016

ABSTRACT

In September and October of 2011, a marine magnetic survey was conducted in the southern East China Sea between 120° and 126°E, 26° and 28°N with the research vessel Kexue-3. New magnetic maps with 5 × 5 km grid spacing were generated after meticulous data processing. Based on an analysis of magnetic anomaly features and further calculation results, including the total horizontal derivatives (THD), second order vertical derivatives (SVD) and analytic signal amplitude (ASA), several new tectonic insights on magnetic sources, basement structures and fault properties were obtained. The NE-SW or NNE-SSW oriented magnetic anomaly highs have different sources: (1) The high amplitude, short wavelength magnetic anomalies of the Zhemin Uplift are caused by shallow buried igneous rocks intruded along NE-NEE oriented faults. (2) The high amplitude, moderate wavelength magnetic anomalies of the Diaoyudao Uplift are caused by the metamorphic basement intruded by magmatic rocks. (3) The magnetic sources of the Yandang Uplift and Taibei Uplift in the shelf basin are shallow buried metamorphic basements and deep buried volcanic bodies, respectively. Several NW-SE or NWW-SEE oriented dextral strike-slip fault belts were identified as important tectonic boundaries. Each is composed of several en echelon and partly overlapping secondary faults. Initially formed in the Cretaceous, these fault belts have evolved through multiple periods, propagated seaward with the migration of the basement rifting and accommodated local stress fields in the Cenozoic.

Keywords: marine magnetic survey, magnetic anomaly, southern East China Sea, basement structures

1. INTRODUCTION

The East China Sea (ECS) is located on the continental margin between the Chinese mainland and the Ryukyu Trench, covering an area of approximately 770000 km^2 (*Zhou et al., 1989*). Topographically, it consists of a wide shelf in the west and the Ryukyu trench-arc-backarc basin system in the east (Fig. 1). Two sedimentary basins (Fig. 2), the East China Sea Shelf Basin (ECSSB) and the Okinawa Trough (OT) bounded by the Taiwan-Sinzi folded belt (or the Diaoyudao Uplift) have developed in this area (*Kong et al., 2000*).

The ECSSB is the largest Cenozoic-Mesozoic oil and gas-bearing basin offshore the eastern Chinese mainland (*Zhou et al., 1989*; *Zhao, 2004*; *Yang et al., 2010*; *Yang, 1992*). Large amounts of marine geological and geophysical surveys and studies have been conducted in the central and northern ECSSB, which have focused primarily on the basin structures, stratigraphy, tectonic evolution and resource potential (*Zhou et al., 1989, 2001*; *Lao et al., 1995*; *Ren et al., 2002*; *Zhao, 2004*; *Yang et al., 2004, 2010*; *Lee et al., 2006*; *Li et al., 2009*; *Cukur et al., 2011*; *Dai et al., 2014*; *Suo et al., 2015*; *Han et al., 2015*). Four

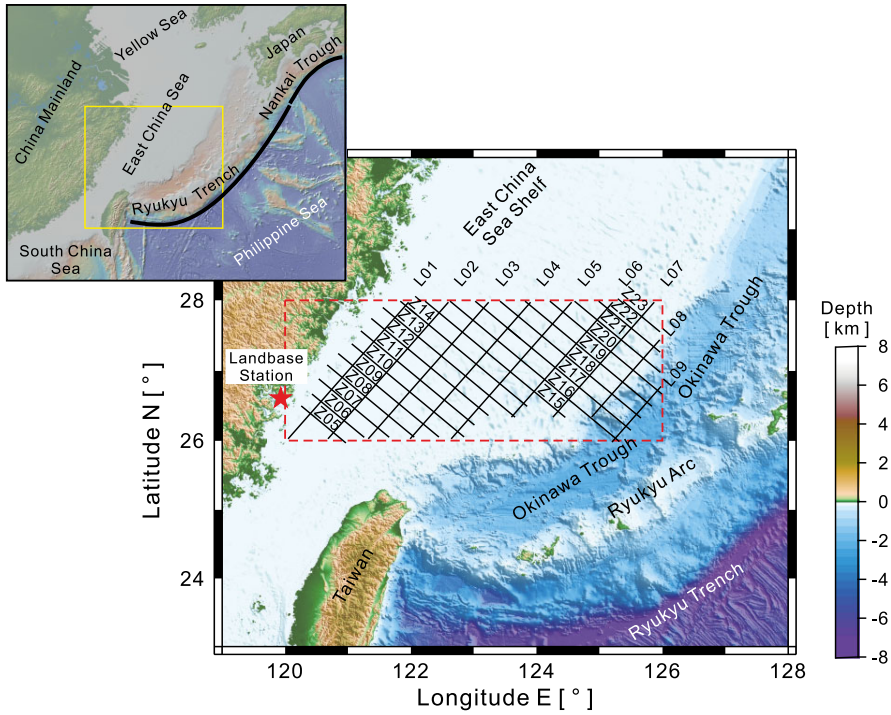

Fig. 1. Location and submarine topography of the southern East China Sea. The yellow rectangle in the inset map denotes the area of the large map. The 2011 surveyed area is outlined by the dashed red rectangle, and the black survey lines are inside it. The red asterisk denotes the land-based station that provided observations of diurnal variations. The bathymetric data are from the Marine Geoscience Data System (*http://www.geomapapp.org/index. htm*).

hydrocarbon-bearing structures have been found and eight oil and gas fields have been developed in the Xihu Depression (*Zhao, 2004; Ye et al., 2007*; *Li et al., 2009*).

In the southern ECSSB, however, less work has been done and the structural characteristics are not fully understood, partly due to political reasons. Well data have revealed that the basement of the southern ECSSB is mainly composed of Proterozoic metamorphic rocks and Mesozoic-Cenozoic igneous rocks (*Liu, 1992*; *Shen et al., 2001*; *Yang et al., 2012*), but the structures and distributions of the two types of basements require further discussion. The existence of thick Mesozoic strata in the deep basin has been suggested (*Li et al., 2012*; *Gong et al., 2014*), but the study of the distribution and thickness of the Mesozoic strata has been hindered due to the shallow penetration of the wells and seismic profiles. Several NW-NWW oriented faults are suggested to extend from the Ryukyu Trench northwestward to the shelf area or even the Chinese mainland and form the main tectonic boundaries in the East China Sea (*Chai et al., 1986*; *Li, 1987a,b*; *Jiao et al., 1988*; *Hsu et al., 1996*; *Kong et al., 2000*; *Hsu et al., 2001*). However, these faults can hardly be traced in the shelf area because they are presently inactive and buried by thick sediments and are thus poorly expressed on seismic profiles.

Marine magnetic data can provide information on subseafloor structures and magnetic sources (*Golynsky et al., 2013*; *Guevara et al., 2013*; *Doo et al., 2015*). In the East China Sea, high magnetic anomalies or high magnetization zones have generally been attributed to basement highs or volcanic rocks (*Hsu et al., 2001*; *Han, 2008*; *Lin et al., 2005*; *Li et al., 2009*), but exceptions such as the low anomaly of the Hupijiao Rise also exist (*Han et al., 2015*). Large-scale fault belts, which separate different structural regions, can also be delineated on magnetic maps (*Jiao et al., 1988*; *Li et al., 2009*). Therefore, a careful examination of the magnetic data can help us further elucidate the structure characteristics of the southern ECSSB and can benefit oil and gas exploration in this area.

In this paper, the 2011 shipborne marine magnetic survey in the southern East China Sea is introduced, and the data processing and magnetic anomaly characteristics are described in detail. On the basis of the above works, several geological problems, such as the poorly known distribution of the magnetic sources and basement properties and the influence of the NW-SE oriented fault belts, are discussed, and new insights are presented.

2. GEOLOGICAL SETTINGS

Three uplift belts and two basins are identified in the East China Sea (Fig. 2) from west to east. They are the Zhemin Uplift, East China Sea Shelf Basin, Diaoyudao Uplift, Okinawa Trough and Ryukyu Arc, which are all parallel or sub-parallel to the Chinese shoreline.

The East China Sea Shelf Basin consists of several depressions separated by basement highs (*Yang, 1992*; *Zhao, 2004*). Underlain by Proterozoic metamorphic rocks and/or Mesozoic- Cenozoic volcanic rocks, there is a 10 km thick Mesozoic-Cenozoic sequence of terrestrial sediments in the basin (*Sun, 1982*; *Ren et al., 2002*; *Cukur et al., 2011*).

The initial extension and rifting of the shelf basin can be traced to the late Cretaceous (*Zhao, 2004*). The structural styles and stratigraphic sequences of different areas contrast strongly (*Yang et al., 2012*), probably due to the seaward migration of the rifting activity since Mesozoic (*Zhao, 2004*; *Suo et al., 2012, 2015*). From the Paleocene to Miocene,

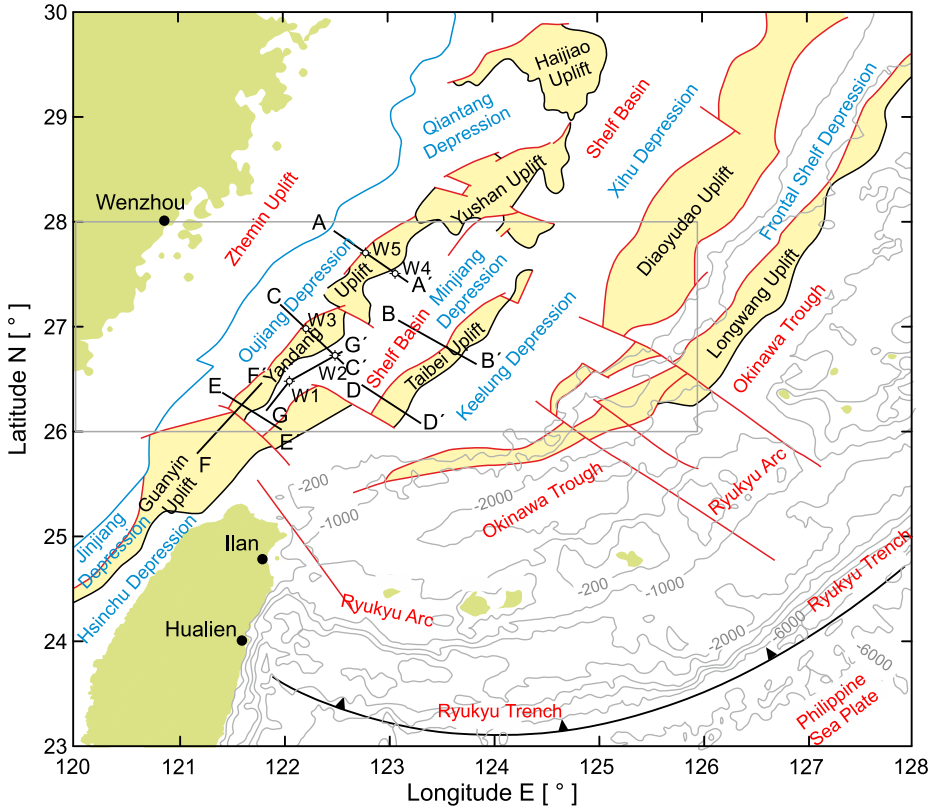

Fig. 2. Structural map of the southern East China Sea and adjacent region (modified from *Kimura, 1985*; *Sibuet et al., 1987*; *Hsu et al., 2001*; *Zhao, 2004*), showing profiles A-A′ to G-G′. The red solid curves represent faults. The basement highs within the Cenozoic basins are yellow colored, and the depressions have blue labels. The survey area of 2011 is outlined by the light gray rectangle. The light gray solid curves are isobaths. The locations of the wells in the shelf basin are denoted by W1 (W1-FZ13-2-1 well), W2 (W2-FZ10-1-1 well), W3 (W3-FZ2-1-1 well), W4 (W4-TB13-1-1 well) and W5 (W5-W26-1-1 well).

multiple uplift-subsidence tectonic cycles produced several unconformities (*Cukur et al., 2011*). The rifting axis of the East China Sea migrated eastward to the Okinawa Trough in the middle-late Miocene, and the shelf basin entered a regional subsidence stage (*Zhao, 2004*).

The Taiwan mountain range to the south of the East China Sea is a young orogenic belt promoted by the collision of the Luzon Arc and Eurasian continental margin (*Teng, 1990a,b*; *Huang et al., 2008*). Influenced by the compressional stress field generated by the collision, the basin geometry and tectonic structures of the southern East China Sea are different from the other parts of the basin.

3. DATA ACQUISITION AND PROCESSING

3.1. Marine geophysical survey

To better understand the national geological setting and reasonably exploit the natural resources, the Chinese government initiated a new round of surveys in 1999 (*Zhang, 2001*). The continental shelf of China has received much attention, and a large amount of work has been performed in the past decade (*Lan et al., 2010*). As powerful tools for the regional tectonic studies, the shipborne magnetic surveys have been widely adopted in Chinese marine geophysical surveys.

An integrated marine geophysical survey was conducted in September and October of 2011 in the area between 120°E and 126°E, 25°N and 28°N using the research vessel Kexue-3 of Institute of Oceanology, Chinese Academy of Sciences (IOCAS). Magnetic data were collected along 28 tracks with a total length over 6000 km (Fig. 1). The spacing of the NW-SE and NE-SW oriented tracks were 25 and 50 km, respectively.

A NAVCOM 2050G system, which had a positioning error of less than 1 m, was used for the DGPS navigation. The total magnetic field was measured using a SeaSPY proton precession magnetometer manufactured by the Marine Magnetics Corporation of Canada. The data were digitally recorded at 1-s intervals. The quality of the raw data was fairly good, and only small amount of distortion and jump-points was found (Fig. 3). A land-based station was established at 26°38′N, 119°59′E in Fujian Province for diurnal observations (Fig. 1). During the period of the geophysical survey, the diurnal variation was stable, and there were no geomagnetic storms (Fig. 4). The data were able to provide effective constraints for diurnal corrections in most parts of the survey area.

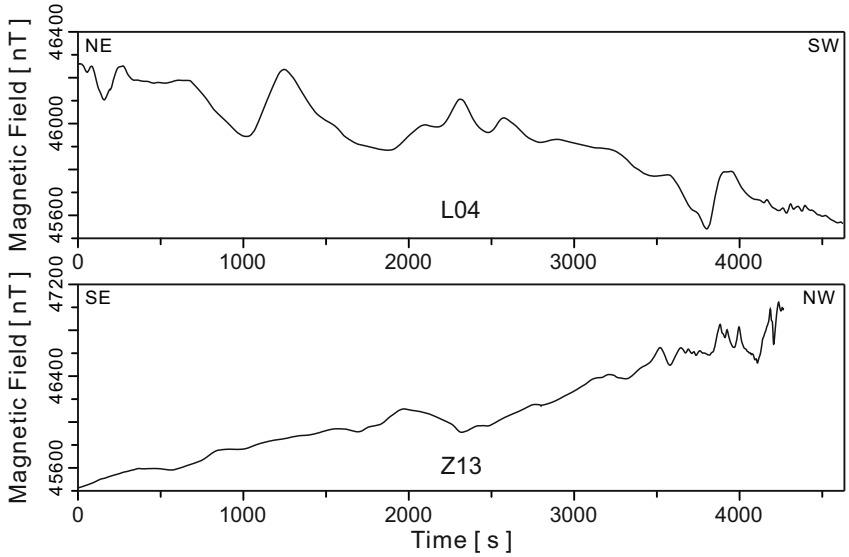

Fig. 3. Measured total magnetic values of survey lines L04 and Z13 shown in Fig. 1.

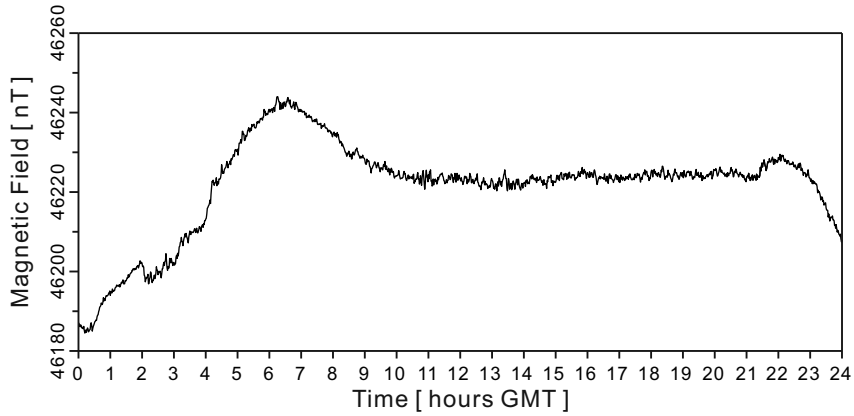

Fig. 4. Typical diurnal variations of total magnetic field recorded by the land-based station on 23 September 2011.

3.2. Data processing

The MMDP software (*Bai et al., 2010*; *Liu et al., 2011*) developed by the China University of Petroleum and the RGIS software (*Zhang, 2011*) developed by the Development Research Center of China Geological Survey were used for the data processing. The raw data set was composed of three independent data groups: navigation, magnetic and diurnal variation. By integrating the first two groups according to time, we obtained the data files of all single tracks that contained both navigation and magnetic data.

Obviously erroneous values generated by equipment were manually deleted. The IGRF-11 model (*Finlay et al., 2010*) was used for the normal field correction, and the diurnal correction was conducted using the land-based station data. Nine-point arithmetical average filtering was applied, and we then obtained the total magnetic anomalies along the tracks.

After the above processing, noise from several resources may still have been present. Because there are no shallow buried volcanic intrusions or extrusions in the survey area, extremely high frequency anomalies were considered to be noise. Wavelet transforms have been suggested as a useful method for reducing noise in magnetic data (*Leblanc and Morris, 2001*; *Zhou et al., 2013*), especially noise generated by ocean waves (*Zhou et al., 2013*). In this study, nine-order 1-D discrete wavelet decomposition was applied to the track data using a db5 wavelet. The first-third order detail coefficients and the third-order approximation coefficients were regarded as noise and magnetic anomaly values, respectively.

Track data adjustment was performed using the half-systematic method (*Huang, 1990*), which is equivalent to the least square method (*Prince et al., 1984*). The mean cross-over errors were finally reduced from 15.1959 nT to 4.8353 nT.

A total magnetic anomaly map of the survey area was generated by gridding the track data into 5×5 km (Fig. 5) using the Kriging method. Magnetic profiles showing the amplitude and wavelength variations along the main tracks were also plotted (Fig. 6).

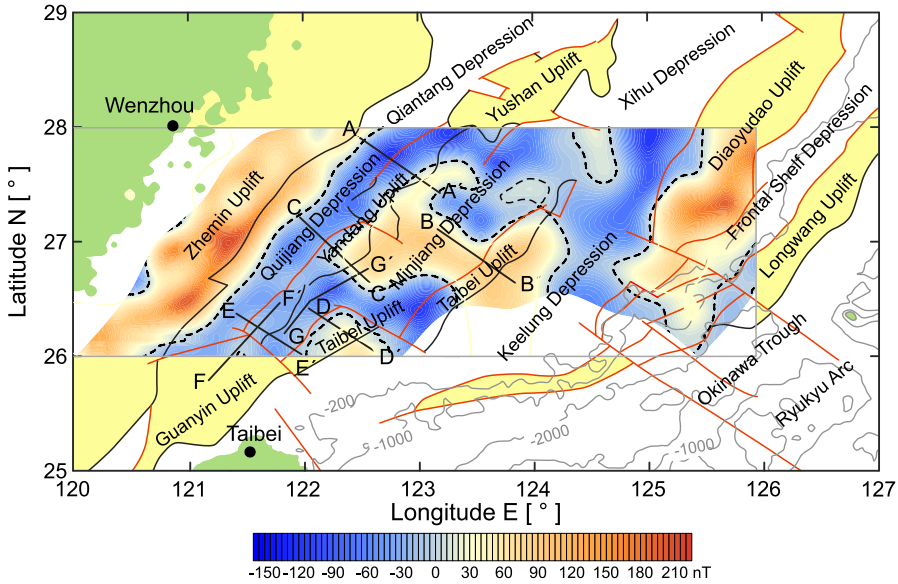

Fig. 5. Total magnetic anomaly of the southern East China Sea, superimposed on a simplified structural map from Fig. 2. Basement uplifts outside the surveyed area are yellow colored. The solid red curves are faults. The dashed black curves are the zero isolines. The positions of seismic profiles A-A′ to G-G′ are shown.

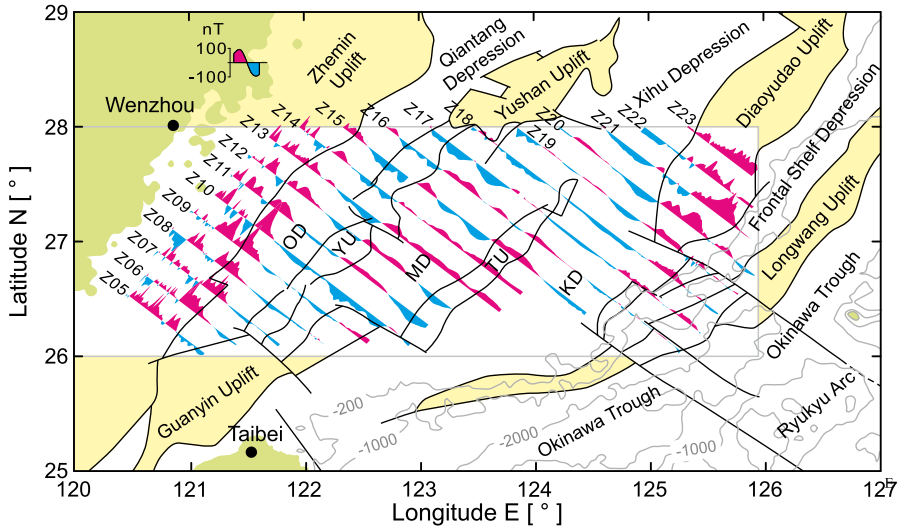

Fig. 6. Magnetic profiles of the NW-SE oriented tracks, superimposed on a simplified structural map from Fig. 2. Basement uplifts outside the surveyed area are yellow colored. The positive and negative anomalies are red and blue colored, respectively. OD-Oujiang Depression, YU-Yandang Uplift, MD-Minjiang Depression, TU-Taibei Uplift, KD-Keelung Depression.

3.3. Reduction to the pole

Influenced by variations of geomagnetic declination and inclination, the magnetization orientations of rocks are rarely vertical but change with their locations, which causes the geological interpretation of magnetic anomalies to be problematic. Reduction to the pole allows the computation of the magnetic anomaly that would be observed if the directions of the magnetization and ambient magnetic field were vertical. According to *Li et al. (2009)*, major tectonic structures such as faults and basement uplifts can be more readily identified from a magnetic map after the reduction than from the original total field magnetic map (*Li et al., 2009*). In addition, the surveyed area is floored mainly with continental crust, and the influence of the magnetic striples that are typical of standard ocean crust need not be considered here (*Hsu et al., 2001*). Because the surveyed area was small and had relatively smooth geomagnetic variations, the geomagnetic parameters (inclination of 39.68° and declination of 4.5°, from the IGRF-11 model) of the center point (123°E, 27°N) were used for the reduction to the pole calculation. The pole-reduced magnetic anomaly is shown in Fig. 7.

4. MAGNETIC ANOMALY FEATURES

To elucidate the tectonic implications of the magnetic anomalies, the basement structure map of the Cenozoic rifting basin obtained primarily by seismic reflection

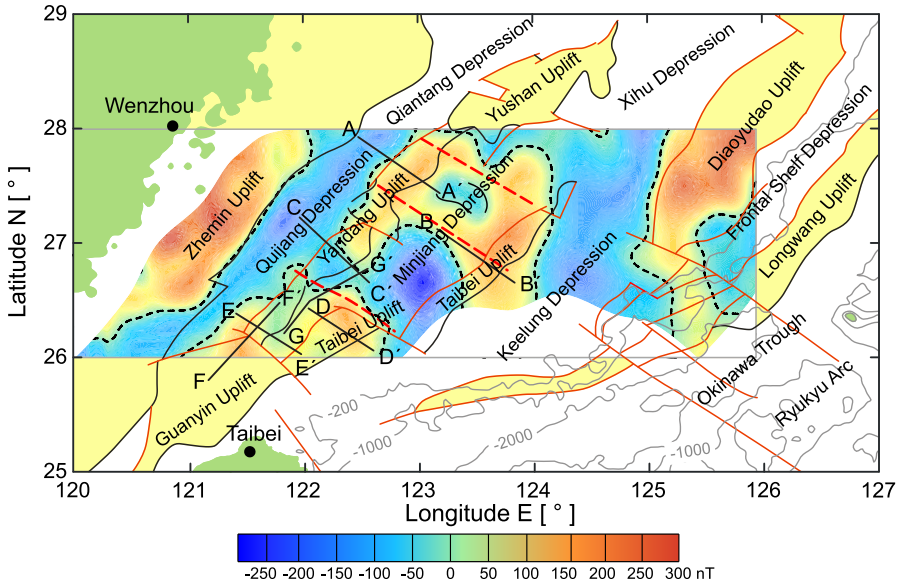

Fig. 7. Reduced-to-the-pole magnetic anomaly of the southern East China Sea, superimposed on a simplified structural map from Fig. 2. Basement uplifts outside the surveyed area are yellow colored. The solid red curves are faults. The dashed black curves are the zero isolines. The bold red dashed lines denote the NW-SE oriented linear features. The positions of seismic profiles A-A′ to G-G′ are shown.

surveys (*Zhao, 2004*; *Yang et al., 2010*; *Lin et al., 2005*) was superimposed on the magnetic anomaly maps (Figs 5–7). As suggested by previous authors (*Hsu et al., 2001*; *Lin et al., 2005*; *Han, 2008*; *Yang et al., 2014*), in the East China Sea, belts with high magnetic anomalies or magnetizations are related to basement highs and/or volcanic belts, whereas belts with low magnetic anomalies and magnetizations are related to depressions.

Alternating magnetic highs and lows oriented NE-SE or NNE-SSW can be seen on the total magnetic anomaly map and pole-reduced magnetic anomaly map. However, the latter can be better correlated with the tectonic map (Fig. 7), suggesting that the reduction to the pole successfully decreased the influence of the oblique magnetization generated by the geomagnetic field.

The pole-reduced magnetic anomaly features can be summarized as follows:

1. The Zhemin Uplift and Oujiang Depression are characterized by high positive and low negative anomalies, respectively.
2. High positive magnetic anomalies are found in the northern part of the Yandang Uplift, whereas negative and low positive anomalies occur in the middle and southern parts.
3. The northernmost Guanyin Uplift and the southernmost Yandang Uplift are characterized by high positive anomalies.
4. A dextral strike-slip fault westerly offsets the southern Taibei Uplift, which has high positively magnetic anomaly for over 50 km. A NNE-SSW oriented high positive anomaly belt covers the northern Taibei Uplift and the northeastern Minjiang Depression.
5. The southern Minjiang Depression and the middle Taibei Uplift are characterized by a low negative anomaly, with a minimum value of approximately –300 nT, which is also the lowest magnetic anomaly in the study area. In the northern Minjiang Depression, two NW-SE oriented linear high magnetic anomaly belts can be observed.
6. The Xihu Depression and Keelung Depression are characterized by low negative magnetic anomalies.
7. The high positive anomaly corresponding to the Diaoyudao Uplift terminates to the south near 27°N. Further south, a NNW-SSE oriented low positive anomaly belt extends into the southern Okinawa Trough. In addition, on the magnetic profiles (Fig. 6), short wavelength anomalies can be observed on the Zhemin Uplift and Diaoyudao Uplift. However, in the Shelf Basin, the wavelengths are relatively long.

5. DISCUSSION: TECTONIC INTERPRETATION OF THE NEW MAGNETIC DATA

Tectonic boundaries, such as faults, unconformities and the edges of intrusions can be identified on gravity and magnetic maps due to the different rock properties or burial depths on the two sides. Gradient zones or abrupt changes in distribution patterns are usually suggested as obvious boundaries. In addition, several techniques including total horizontal derivatives (*Cordell and Grauch, 1985*; *Grauch and Cordell, 1987*; *Wang, 2010a*), vertical derivatives (*Evjen, 1936*; *Henderson and Zietz, 1949*; *Wang et al., 2010b*;

Hood and McClure, 1965; *Hood and Teskey, 1989*; *Zhong et al., 2007*), analytic signal amplitude (*Nabighian, 1972*; *Roset et al., 1992*; *Qin, 1994*; *Debeglia and Corpel, 1997*; *Li, 2006*), tilt angle (*Miller and Singh, 1994*), theta map (*Wijins et al., 2005*) and enhanced analytic signal (*Hsu et al., 1996a*), have been proposed and proved to be effective methods for the detection of geological boundaries from potential field data.

In this work, the total horizontal derivatives (THD), second-order vertical derivatives (SVD) and analytic signal amplitude (ASA) methods were applied to the pole-reduced magnetic data. The maxima of the THD lie above the top edges when the magnetic source is buried extremely shallowly (for example, the depth/width ratio is less than 0.1) but shift outward as the source depth increases (*Wang et al., 2010a*). A similar variation law is applicable to the zero points of the SVD (*Wang et al., 2010b*). Conversely, the maxima of the ASA shift from the edges inward to the center of the magnetic source as the burial depth increases (*Li, 2006*). According to the seismic profiles, we regard the magnetic sources of the Zhemin Uplift and Shelf Basin as having shallow and deep burial depths, respectively, and will use the THD (Fig. 8), SVD (Fig. 9) and ASA (Fig. 10) calculation results to discuss the basement structures.

5.1. Magnetic sources and basement properties

The East China Sea Shelf Basin is the largest Cenozoic-Mesozoic sedimentary basin in the offshore area of the east Eurasian continental margin (*Zhao, 2004*). The basement is mainly composed of Mesozoic-Paleozoic metamorphic and Mesozoic-Cenozoic volcanic rocks (*Liu, 1992*; *Shen et al., 2001*; *Yang et al., 2012*), and some Proterozoic paleobasement highs also exist (*Wu and Liu, 1992*). Well and seismic data suggest that the Mesozoic strata are widely distributed in the southern East China Sea, but the thickness varies greatly due to the differential uplift and erosion histories in the different areas (*Li et al., 2012*; *Yang et al., 2014*). Although the distribution pattern of the pole-reduced magnetic anomaly is fairly consistent with the tectonic framework of the pre-Cenozoic basement as revealed by seismic data (Fig. 7), some discrepancies are still exist locally.

Seismic reflection profiles have revealed that the basement depth of the Zhemin Uplift is shallower than 1 km and that a series of NE-SW oriented normal faults developed on it (*Suo et al., 2015*). Farther west, on the nearby land, Cenozoic-Mesozoic volcanic rocks are widely distributed in the Fujian and Zhejiang Provinces (*Yang et al., 2012*; *Suo et al., 2015*). We postulate that the offshore high amplitude, short wavelength magnetic anomalies are generated by shallow buried volcanic rocks. The SVD map (Fig. 9) shows that a narrow NE-SW oriented positive belt lies on the eastern margin of the Zhemin Uplift, which can be attributed to the intrusions along the active Binhai Fault (*Huang and Wang, 2006*). The fault belt forms the boundary between the Zhemin Uplift and Oujiang Depression and can be seen as high positive anomalies on the THD and ASA maps. Other positive features in this area, although discontinuous, are also aligned in the NE-SW direction on the SVD map, in agreement with the fact that the onshore volcanic rocks are distributed along NE-NEE oriented faults (*Yang et al., 2012*). Accordingly, we suggest that the volcanic rocks intruded along the NE-SW oriented fault belts are the main magnetic sources of the high amplitude, short wavelength anomalies on the Zhemin Uplift (Fig. 6).

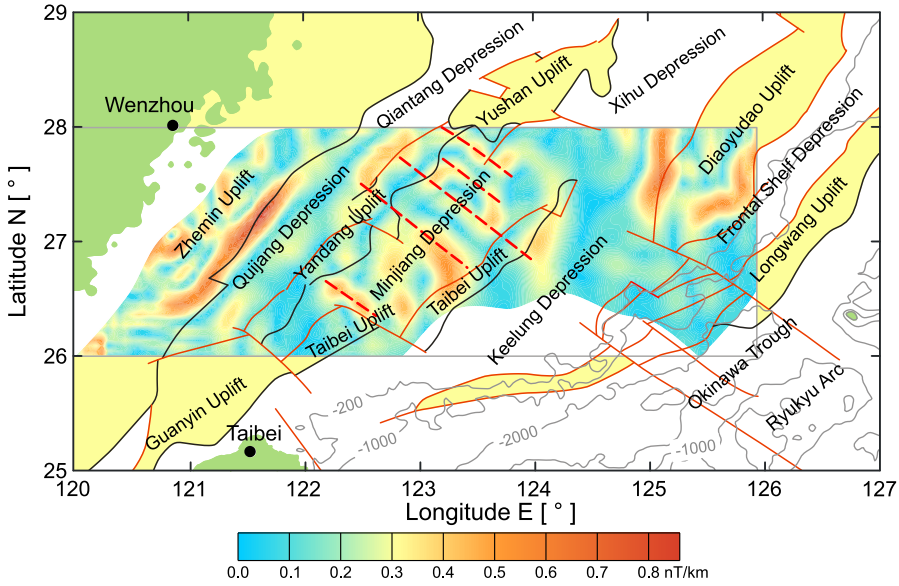

Fig. 8. Total horizontal derivatives of the reduced-to-the-pole magnetic anomaly, superimposed on a simplified structural map from Fig. 2. Basement uplifts outside the surveyed area are yellow colored. The solid red curves are faults. The dashed bold red lines denote the NW-SE oriented linear features.

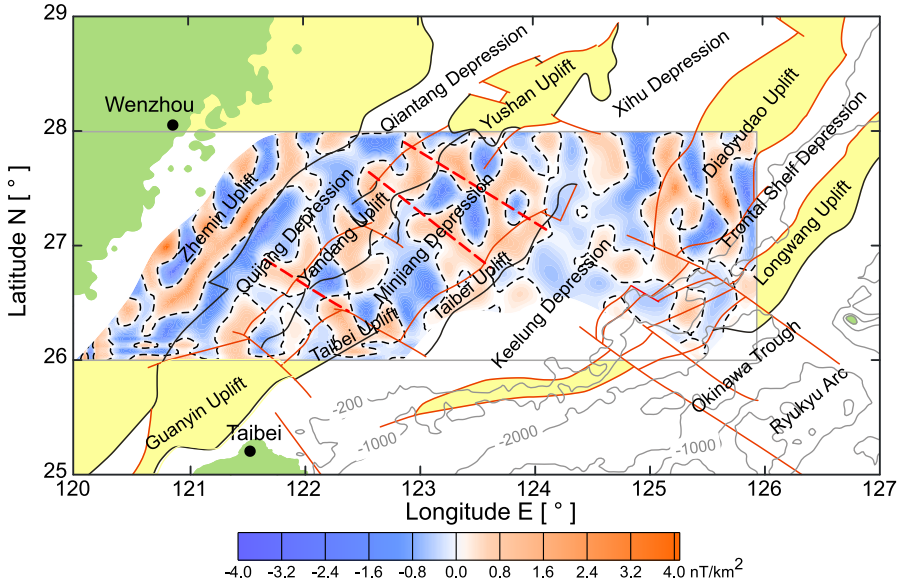

Fig. 9. The same as in Fig. 8, but for the second-order vertical derivatives.

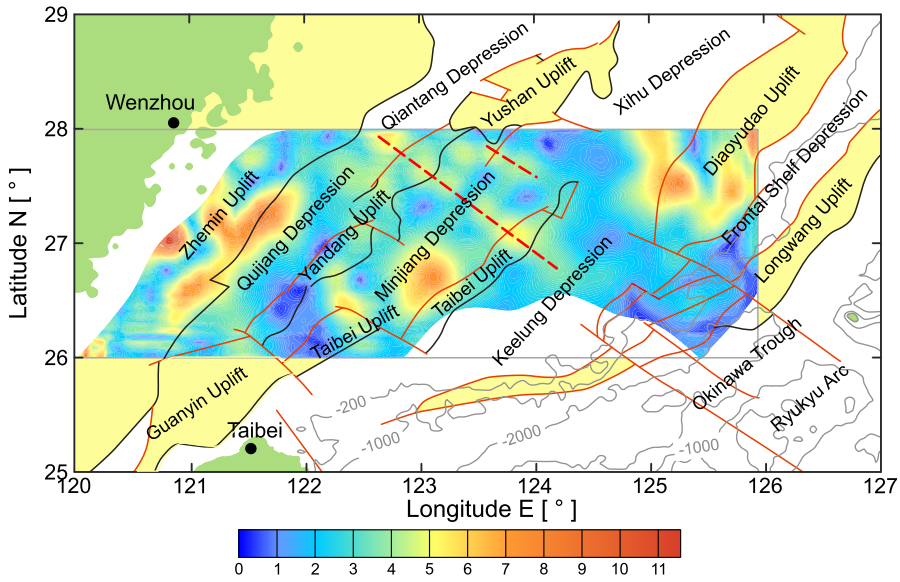

Fig. 10. The same as in Fig. 8, but for the analytic signal amplitude.

Low amplitude and long wavelength anomalies in the shelf basin (Fig. 6) indicate a weak magnetization and/or large burial depth of the magnetic sources. The pre-Mesozoic basement of the southern Yandang Uplift is buried more deeply and is overlain by thicker Mesozoic strata compared with the northern part (*Li et al., 2012*; *Yang et al., 2014*). Taking into account the relatively high and low magnetic anomalies of the northern and southern Yandang Uplift (Fig. 7), respectively, we propose that the pre-Mesozoic metamorphic rocks are the main magnetic sources. Magmatic intrusions were found near the northern Yandang Uplift (*Yang et al., 2014*), and the THD maxima suggest that the igneous rocks are mainly distributed along the fault between the northern Yandang Uplift and the Oujiang Depression (Fig. 8).

The northern Taibei Uplift is well delineated by the zero points of the SVD (Fig. 9) but is not distinct on the THD (Fig. 8) and ASA (Fig. 10) maps. The seismic profiles (Fig. 11) and well data suggest that the Taibei Uplift is mainly composed of intermediate-acid igneous rocks (*Li et al., 2012*; *Yang et al., 2012*). At the boundary of the Mesozoic and Cenozoic, intense magmatic activities deformed and truncated the pre-existing Mesozoic strata in this area (*Suo et al., 2012, 2015*). Consequently, the eastern shelf basin was subdivided into two parts by the emplaced igneous bodies: the Minjiang Depression to the west and the Keelung Depression to the east. The relatively weak magnetization of the rocks combined with large burial depths produced the low amplitude, long wavelength magnetic anomalies of the Taibei Uplift. Therefore, despite the similar magnetic anomaly characteristics, the magnetic sources of the Yandang and Taibei uplifts are essentially different from each other.

The high positive magnetic anomaly of the Diaoyudao Uplift terminates to the south at 27°N and two N-S oriented maximum belts can be identified (Fig. 7). The wavelength of the magnetic anomalies is longer than those of the Zhemin Uplift (Fig. 6). Seismic profiles revealed that the basement of the Diaoyudao Uplift is wide and is composed of predominantly pre-Miocene metamorphic rocks intruded by Miocene and pre-Miocene magmatic rocks (*Gungor et al., 2012*; *Shang, 2014*). Pliocene and Quaternary strata overlie the basement, but some remnant Miocene strata also exist locally (*Gungor et al.,*

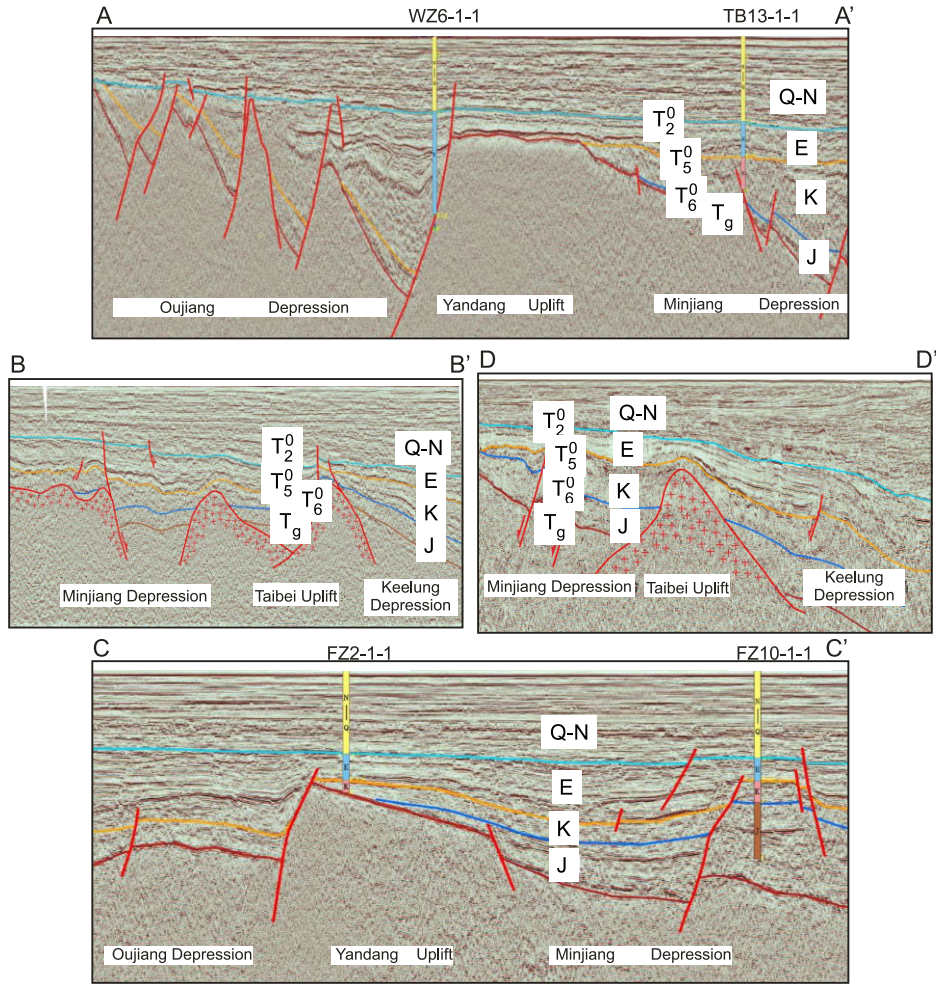

Fig. 11. Seismic reflection profiles in the southern East China Sea (from *Li et al., 2012*). The yellow bars are the wells. For the locations of the profiles and wells, see Fig. 2. The names of the tectonic units are shown at the bottom. Labels Q-N, E, K and J are stratigraphic units separated by the seismic reflectors (T_2^0 , T_5^0 , T_6^0 and T_g): Q-N: Quaternary and Neogene; E: Eocene (E1 and E2 represent the upper and lower parts, respectively); K: Cretaceous; J: Jurassic.

2012; *Shang, 2014*). The magnetic data concur with the seismic data. The magmatic-intruded metamorphic basement generated the high amplitude, long wavelength anomalies which can be decomposed into low amplitude, long wavelength anomalies generated by the metamorphic rocks and high amplitude, short wavelength anomalies generated by the volcanic rocks.

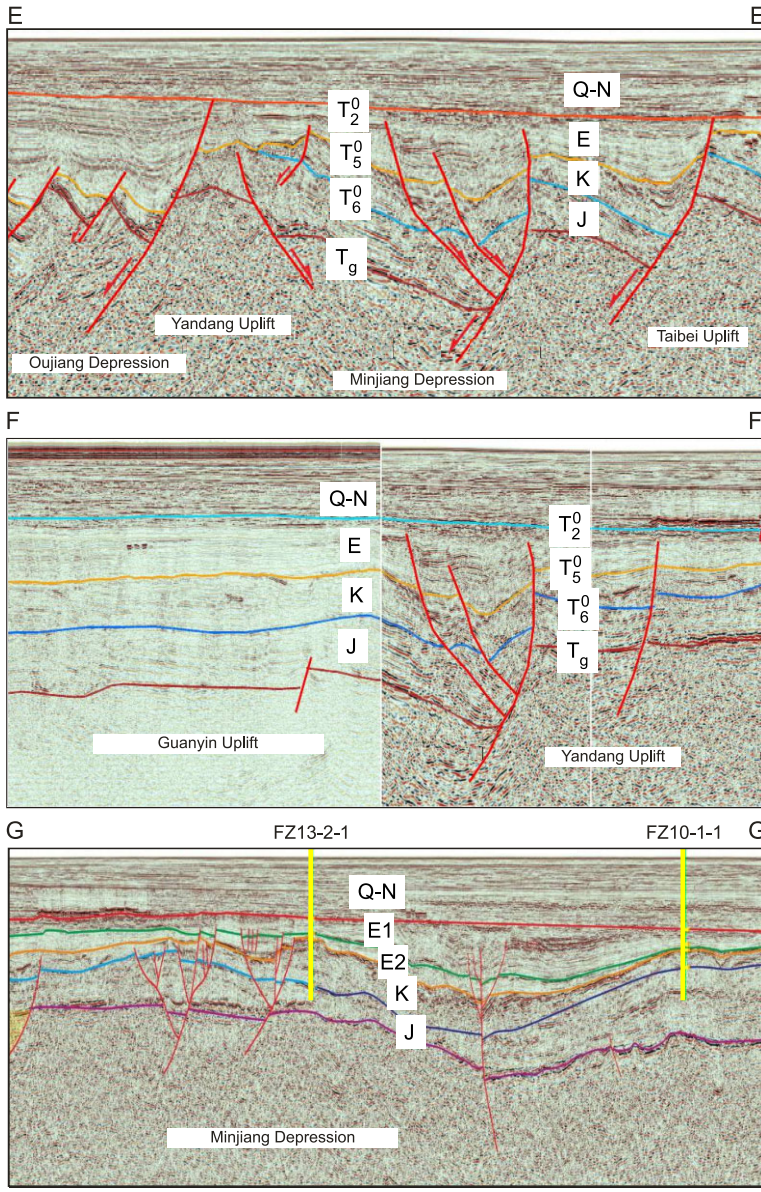

Fig. 11. Continuation.

5.2. NW-SE oriented faults

The Kula, Pacific and Philippine Sea plates have been subducting under the Eurasian plate successively since the Mesozoic, and the tectonic framework near the plate boundary has changed drastically. Numerous NW-SE or NWW-SEE oriented strike-slip faults developed near the eastern Eurasian margin. A large mount of work has been performed by previous authors (*Chai, 1986*; *Li, 1987a,b*; *Jiao, 1988*; *Hsu, 1996b, 2001*; *Kong et al., 2000*). *Li (1987a,b)* suggested that these faults are uniformly spaced and of dextral strike-slip type, extend from the Ryukyu Arc northwestward to the shelf or even onshore area and accommodated the stress field variations in the East China Sea. Based on calculations of equivalent magnetization, *Hsu et al. (2001)* suggested that the Miyako fault belt, which corresponds to the Miyako-Yandang high magnetization zone, is the tectonic boundary of the middle and southern Okinawa Trough. *Hsu et al. (1996b)* and *Kong et al. (2000)* suggested that several NW-SE oriented dextral strike-slip faults generated by the Taiwan mountain building process exist in the southern Okinawa Trough and northeastern Taiwan.

The NW-SE oriented fault belts are well expressed by topography, gravity anomalies and seismic reflections in the arc and back arc basin regions (*Li, 1987a,b*). On seismic profiles of the shelf margin, the faults correspond to negative flower structures (*Kong et al., 2000*; *Shang, 2014*). However, in the shelf basin area, they only developed in the deeply buried pre-Miocene strata and the basement. Thus, the shallow penetration seismic reflection profiles cannot reveal the faults in detail. However, the locations and geometry of the fault belts can be traced by magnetic anomalies that are more sensitive to the rock property changes. Several criteria can be used to identify the strike-slip faults on the magnetic anomaly map. Large strike-slip faults generally offset magnetic anomaly belts laterally. Linear high positive anomalies associated with magmatic intrusions are generally distributed along deep-seated strike-slip faults because the melts usually upwell along fracture zones. Basement contrasts on the two sides caused by large lateral displacement combined with possible vertical displacements associated with pull-apart or compression activities can form obvious gradient zones along the faults.

In the study area, although the magnetic highs are predominantly NE-SW oriented, several NW-SE oriented features can be identified, especially in the shelf basin area (Fig. 7). Two NWW-SEE oriented positive magnetic anomaly belts exist in the Minjiang Depression at 27°N and 27.5°N. The seismic reflection data (Fig. 11) suggest that there is no detective basement high in this area, and we therefore postulate that the two belts were generated by the igneous rocks that intruded along the two NWW-SEE oriented fault belts. South of the Minjiang Depression, the fault dextrally offsetting the Taibei Uplift is corresponds to a NWW-SEE oriented gradient zone, with magnetic values that decrease northeastward.

Similar features can also be found on the free-air gravity anomaly map (Fig. 12). Three main linear belts can be identified. The southern belt corresponds to a gradient zone with gravity anomaly values that decrease northeastward. The middle and northern belts correspond to high positive anomaly belts that separate the different anomaly patterns on the two sides. The positions of these linear features are in agreement with those on the magnetic map (Fig. 7).

The calculated THD, SVD and ASA results enhance the appearances of the linear features (Figs 8–10). A series of NW-SE or NWW-SEE oriented high positive belts can be seen. Due to the large burial depth of the basement and a lack of knowledge of its precise depth over most of the shelf basin, the linear features do not precisely correspond to the actual structure boundaries, and it was difficult for us to determine the displacements between them. However, we are able to roughly demarcate the structural boundaries by correlating the different maps because the belts are relatively narrow (Figs 8–10).

As mentioned above, NW-SE or NWW-SEE oriented faults in the East China Sea have been identified by previous authors in the Okinawa Trough, beneath the shelf margin and on the uplifts of the shelf basin (Fig. 2) (*Li, 1987a,b*; *Hsu et al., 1996b*; *Kong et al., 2000*; *Shang et al., 2016*). The linear features on the magnetic and gravity maps are coincident with or are the extensions of existing faults, prompting us to propose that they represent the deeply buried NW-SE or NWW-SEE oriented dextral strike-slip faults.

Because most of the NW-SE or NWW-SEE oriented linear features are discontinuous and have lateral offsets, we postulate that single fault belts may be composed of several en echelon and partly overlapping secondary faults, which may have developed in multiple stages as proposed by *Li (1987a,b)*. The shear stress field generated by the convergence of the Pacific and Eurasian plates promoted the formation of transverse fault belts during the initial rifting of the ECSSB in the Cretaceous. They were strike-slip faults, and some of them were possibly transform faults that extended southeastward to the plate boundary. In

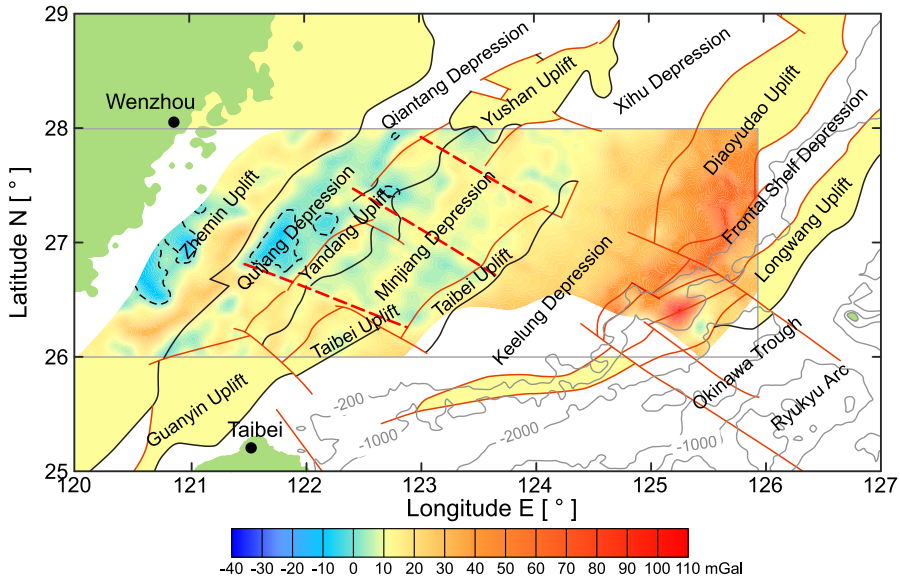

Fig. 12. Free-air gravity anomaly map of the southern East China Sea, superimposed on a simplified structural map from Fig. 2. Basement uplifts outside the surveyed area are yellow colored. The solid red curves are faults. The dashed black curves are the zero isolines. The dashed bold red lines denote the NW-SE oriented linear features.

the Cenozoic, the transverse faults propagated with the seaward migration of the rifting activity and accommodated the local stress fields. Since the Miocene, induced by the Taiwan mountain building process, the compressional stress field direction of the southern Ryukyu trench-arc-back arc system has changed from NW to NNW-NS. Consequently, the strikes of the fault belts near Taiwan have rotated clockwise relative to the northern faults.

In general, the NW-NWW oriented transverse fault belts are important tectonic boundaries that separate different blocks of the southern East China Sea. However, additional work, especially deep seismic surveys, are needed to further elucidate the detailed characteristics of the fault belts.

6. CONCLUSIONS

As part of a land and resources survey promoted by the Chinese government, the 2011 marine magnetic survey in the southern East China Sea has been introduced in detail. The raw data were processed carefully, and the total magnetic anomaly and pole-reduced magnetic anomaly were obtained. On the basis of a qualitative analysis of the magnetic anomaly, combined with further calculations such as the total horizontal derivatives (THD), second-order vertical derivatives (SVD) and analytic signal amplitude (ASA), several tectonic problems were discussed and some new insights on basement structures were given.

NE-SW or NNE-SSW oriented high positive magnetic anomaly belts exist in the southern East China Sea. The high amplitude, short wavelength magnetic anomalies of the Zhemin Uplift are generated by shallow buried igneous rocks intruded along NE-NEE oriented faults. The high amplitude, moderate wavelength magnetic anomalies of the Diaoyudao Uplift are generated by the magmatic-intruded metamorphic basement and can be decomposed into low amplitude, long wavelength anomalies generated by the metamorphic rocks and high amplitude, short wavelength anomalies generated by the magmatic rocks. The two positive anomaly belts in the shelf basin, although having similar amplitudes and wavelengths, are generated by different sources. The magnetic sources of the Yandang Uplift to the west and the Taibei Uplift to the east are a shallow buried metamorphic basement and deep buried volcanic bodies, respectively.

Several NW-SE or NWW-SEE oriented strike-slip fault belts can be traced in the shelf basin by correlating the linear features on magnetic and gravity maps. As the main tectonic boundaries, each of these fault belts are found to be composed of several en echelon and partly overlapped secondary faults. Initially formed in the Cretaceous, these fault belts have propagated with the seaward migration of the rifting activities and have accommodated the local stress field variations. More work, especially deep seismic detections, is needed to further elucidate the detailed characteristics of these fault belts.

Acknowledgements: This study was funded by the National Key Basic Research Program of China (973 Program; Grant No. 2013CB429701) and the National Natural Science Foundation of China (Grant No. 41506080). The authors wish to thank research assistant Wei Geng of QIMG (Qingdao Institute of Marine Geology) for providing data. We also would like to thank engineer Zhaodai Zhang of QIMG and Dr. Yongliang Bai of IOCAS for helping with the data processing.

References

Bai Y.L., Liu Z., Zhang Z.X., Yang H. L., Zhang G., Shi Z.Y. and Du R.L., 2010. Marine magnetic data processing technology and software realization. *Ocean Technol.*, **29(4)**, 34–37 (in Chinese).

Chai L.G., 1986. The nature of Yushan-Kume fault belt and its control over East China Sea. *Oil Gas Geol.*, **7(2)**, 107–115 (in Chinese).

Cordell L. and Grauch V.J.S., 1985. Mapping basement magnetization zones from aeromagnetic data in the San Juan Basin, New Mexico. In: Hinze W.J. (Ed.), *The Utility of Regional Gravity and Magnetic Anomaly Maps*. Society of Exploration Geophysicists, Tulsa, OK, 181–197.

Cukur D., Horozal S., Lee G.H., Kim D.C., Han H.C. and Kang M.H., 2011. Structural evolution of the northern East China Sea Shelf Basin interpreted from cross-section restoration. *Mar. Geophys. Res.*, **32**, 363–381.

Dai L.M., Li S.Z., Lou D., Liu X., Suo Y.H. and Yu S., 2014. Numerical modeling of Late Miocene tectonic inversion in the Xihu Sag, East China Sea Shelf Basin, China. *J. Asian Earth Sci.*, **86**, 25–37.

Debeglia N. and Corpel J., 1997. Automatic 3-D interpretation of potential field data using analytic signal derivatives. *Geophysics*, **62**, 87–96.

Doo W.B., Hsu S.K. and Armada L., 2015. New magnetic anomaly map of the East Asia with some preliminary tectonic interpretations. *Terr. Atmos. Ocean. Sci.*, **26**, 73–81.

Evjen H.M., 1936. The place of the vertical gradient in gravitational interpretations. *Geophysics*, **1**, 127–136.

Finlay C.C., Maus S., Beggan C.D., Bondar T.N., Chambodut A., Chernova T.A., Chulliat A., Golovkov V.P., Hamilton B., Hamoudi M., Holme R., Hulot G., Kuang W., Langlais B., Lesur V., Lowes F.J., Lühr H., Macmillan S., Mandea M., McLean S., Manoj C., Menvielle M., Michaelis I., Olsen N., Rauberg J., Rother M., Sabaka T.J.9, Tangborn A., Tøffner-Clausen L., Thébault E., Thomson A.W.P., Wardinski I., Wei Z. and Zvereva T.I., 2010. International Geomagnetic Reference Field: the eleventh generation. *Geophys. J. Int.*, **183**, 1216–1230.

Golynsky A.V., Ivanov S.V., Kazankov A.J., Jokat W., Masolov V.M., von Frese R.R.B. and the ADMAP Working Group, 2013. New continental margin magnetic anomalies of East Antarctica. *Tectonophysics*, **585**, 172–184.

Gong J.M., Xu L.M., Yang Y.Q., Li G., Deng K. and Jiang Y.B., 2014. Discussion on Mesozoic hydrocarbon potential of southern East China Sea based on comparison between offshore and onshore areas. *Global Geol.*, **33(1)**, 171–177 (in Chinese).

Grauch V.J.S. and Cordell L., 1987. Limitation of determining density or magnetic boundaries from the horizontal gradient of gravity or pseudo-gravity data. *Geophysics*, **52**, 118–121.

Guevara N.O., Garcia A. and Arnaiz M., 2013. Magnetic anomalies in the Eastern Caribbean. *Int. J. Earth Sci.*, **102**, 591–604.

Gungor A., Lee G.H., Kim H.J., Han H.C., Kang M.H., Kim J.H. and Sunwoo D., 2012. Structural characteristics of the northern Okinawa Trough and adjacent areas from regional seismic reflection data: Geological and tectonic implications. *Tectonophysics*, **522–523**, 198–207.

Han B., 2008. *Geophysical Field and Deep Tectonic Features of East China Sea*. PhD Thesis. Institute of Oceanology, Chinese Academy of Sciences, Qingdao, China (in Chinese).

Han H. C., Lee Y.S., Hwang J.S., Lee S.G., Yoon Y. and Stagpoole V., 2015. Geophysical characteristics of the Hupijiao Rise and their implication to Miocene volcanism in the northeastern part of the East China Sea. *Mar. Geol.*, **363**, 134–145.

Henderson R.G. and Zietz I., 1949. The computation of second vertical derivatives of geomagnetic fields. *Geophysics*, **14**, 508–516.

Hood P. and McClure D.J., 1965. Gradient measurements in ground magnetic prospecting. *Geophysics*, **30**, 403–410.

Hood P.J. and Tesky D.J., 1989. Aeromagnetic gradiometer program of the Geological Survey of Canada. *Geophysics*, **54**, 1012–1022.

Hsu S.K., 2001. Magnetic inversion in the East China Sea and Okinawa Trough: Tectonic implications. *Tectonophysics*, **333**, 111–122.

Hsu S.K., Sibuet J.C. and Shyu C.T., 1996a. High-resolution detection of geologic boundaries from potential-field anomalies: An enhanced analytic signal technique. *Geophysics*, **61**, 373–386.

Hsu S.K., Sibuet J.C., Monti S., Shyu C.T. and Liu C.S., 1996b. Transition between the Okinawa Trough backarc extension and the Taiwan collision: New insight on the southernmost Ryukyu subduction zone. *Mar. Geophys. Res.*, **18**, 163–187.

Huang C.Y., Chien C.W., Yao B.C. and Chang C.P., 2008. The Lichi mélange: A collision mélange formation along early arcward backthrusts during forearc basin closure, Taiwan arc-continent collision. *Geol. Soc. Amer. Spec. Paper*, **436**, 127–154.

Huang M.T., 1990. Examination, adjustment and precision estimation of half-systematic error in marine gravity surveying. *Mar. Sci. Bull.*, **9(4)**, 81–86 (in Chinese).

Huang Z. and Wang S.X., 2006. Tectonic features and activity of Binhai fault zone in Taiwan Strait. *J. Geodesy Geodyn.*, **26(3)**, 16–22 (in Chinese).

Jiao R.C., 1988. On properties of Zhoushan-Guotou fault zone and its extension towards the continent. *Geophys. Geochem. Explor.*, **12(4)**, 249–255 (in Chinese).

Kimura M., 1985. Back-arc rifting in the Okinawa Trough. *Mar. Pet. Geol.*, **2**, 222–240.

Kong F.C., Lawver L.A. and Lee T.Y., 2000. Evolution of the southern Taiwan-Sinzi Folded Zone and opening of the southern Okinawa Trough. *J. Asian Sci.*, **18**, 325–341.

Lan X.H., Zhang Z.X., Li R.H., Yang H.L. and Lu K., 2010. Current status and problems of basic marine geological survey. *Mar. Geol. Lett.*, **26(10)**, 40–44 (in Chinese).

Lao Q. and Zhou Z., 1995. Geological history of the East China Sea. In: *Proceedings of the Third International Conference on Asian Marine Geology, Cheju, October 17-21*. Korean Society of Oceanography, South Korea.

Leblanc G.E. and Morris W.A., 2001. Denoising of aeromagnetic data via the wavelet transform. *Geophysics*, **66**, 1793–1804.

Lee G.H., Kim B., Shin K.S. and Sunwoo D., 2006. Geologic evolution and aspects of the petroleum geology of the northern East China Sea shelf basin. *AAPG Bull.*, **90**, 237–260.

Li C.F., Chen B. and Zhou Z.Y., 2009. Deep crustal structures of eastern China and adjacent seas revealed by magnetic data. *Sci. China Ser. D Earth Sci.*, **52**, 984–993.

Li G., Gong J.M., Yang C.Q., Yang C.S., Wang W.J., Wang H.R. and Li S.Z., 2012. Stratigraphic feature of the Mesozoic "Great East China Sea"-A new exploration field. *Mar. Geol. Quat. Geol.*, **32(3)**, 98–104 (in Chinese).

Li N.S., 1987a. Approaching the submarine faults of the Okinawa Trough on the basis of gravity data. *Mar. Sci.*, **6**, 11–16 (in Chinese).

Li N.S., 1987b. On the fracturing structures of the Okinawa Trough. *Oceanol. Limnol. Sinica*, **19(4)**, 347–358 (in Chinese).

Lin J.Y., Sibuet J.C. and Hsu S.K., 2005. Distribution of the East China Sea continental shelf basins and depths of magnetic sources. *Earth Planets Space*, **57**, 1063–1072.

Liu G.D., 1992. *Geologic-Geophysics Features of China Seas and Adjacent Regions*. Science Press, Beijing, China (in Chinese).

Liu Z., Bai Y.L., Zhang Z.X., Yang H.L., Du R.L., Shi Z.Y. and Zhang G., 2011. Marine magnetic data processing technology and software realization. *Mar. Geol. Front.*, **27(9)**, 60–64 (in Chinese).

Li X., 2006. Understanding 3D analytic signal amplitude. *Geophysics*, **71(2)**, 13–16.

Miller H.G. and Singh V., 1994. Potential field tilt- a new consept for location of potential sources. *J. Appl. Geophys.*, **32**, 213–217.

Nabighian M.N., 1972. The analytical signal of two-dimensional magnetic bodies with polygonal cross-section: its properties and use for automated anomaly interpretation. *Geophysics*, **37**, 507–517.

Prince R.A. and Forsyth D.W., 1984. A simple objective method for minimizing crossover errors in marine gravity data. *Geophysics*, **49**, 1070–1083.

Qin S., 1994. An analytic signal approach to the interpretation of total magnetic anomalies. *Geophys. Prospect.*, **42**, 665–675.

Ren J.Y., Tamaki K., Li S.T. and Zhang J.X., 2002. Late Mesozoic and Cenozoic rifting and its dynamic setting in Eastern China and adjacent areas. *Tectonophysics*, **344**, 175–205.

Roset W.R., Verhoef J. and Pilkington M., 1992. Magnetic interpretation using the 3-D analytic signal. *Geophysics*, **57**, 116–125.

Shang L.N., 2014. *Tectonics and Evolution of the Okinawa Trough*. PhD Thesis. Ocean University of China, Qingdao, China (in Chinese).

Shang L.N., Zhang X.H., Han B. and Du R.L., 2016. On the tectonic problems of the southern East China Sea and adjacent regions: Evidence from gravity and magnetic data. *J. Ocean Univ. China*, **15**, 93–106.

Shen R.Q., Li S.Q. and Xie R.H., 2001. *Magmatic Activity of the East China Sea*. Geological Publishing House, Beijing, China.

Sibuet J.C., Letouzey J., Barrier F., Charvet J., Foucher J.P., Hilde T.W.C., Kimura M., Chiao L.Y., Marsset B., Muller C. and Stephan J.F., 1987. Back arc extension in the Okinawa Trough. *J. Geophys. Res.*, **92(B13)**, 14041–14063.

Sun S.C., 1982. The Tertiary basin offshore Taiwan. In: Saldivar-Sali A. (Ed.), *Proceedings of the Second ASCOPE Conference and Exhibition, October 7-11, 1981, Manila, Philippines*. Metro Manila, Philippines: ASCOPE, ASEAN Council on Petroleum, 126–135.

Suo Y.H., Li S.Z., Dai L.M., Liu X. and Zhou L.H., 2012. Cenozoic tectonic migration and basin evolution in East Asia and its continental margins. *Acta Petrol. Sinica*, **28**, 2602–2618.

Suo Y.H., Li S.Z., Zhao S.J., Somerville I.D., Yu S., Dai L.M., Xu L.Q., Cao X.Z. and Wang P.C., 2015. Continental margin basins in East Asia: tectonic implications of the Meso-Cenozoic East China Sea pull-apart basins. *Geol. J.*, **50**, 139–156.

Teng L.S., 1990a. Geotectonic evolution of late Cenozoic arc-continent collision in Taiwan. *Tectonophysics*, **183**, 57–76.

Teng L.S., 1990b. Extensional collapse of the northern Taiwan mountain belt. *Geology*, **24**, 949–952.

Wang W.Y., 2010a. Spatial variation law of the extreme value positions of total horizontal derivative for potential data. *Chinese J. Geophy.*, **53**, 2257–2270 (in Chinese).

Wang W.Y., Zhang G.C. and Liang J.S., 2010b. Spatial variation low of vertical derivative zero points for potential field data. *Appl. Geophys.*, **7(3)**, 197–209.

Wijins C., Perez C. and Kowalczyk P., 2005. Theta map: Edge detection in magnetic data. *Geophysics*, **70(4)**, 39–43.

Wu H.Z. and Liu Y.Z., 1992. Magnetic field characteristics of the East China Sea Shelf area. In: Liu G.D. (Ed.), *Geologic-Geophysics Features of China Seas and Adjacent Regions*. Science Press, Beijing, China, 118–123 (in Chinese).

Yang C.S., Li G., Yang C.Q., Gong J.M. and Liao J., 2012. Temporal and spatial distribution of the igneous rocks in the East China Sea Shelf Basin and its adjacent regions. *Mar. Geol. Quat. Geol.*, **32(3)**, 125–133 (In Chinese).

Yang C.S., Li G., Luang X.W., Yang C.Q., Gong J.M., Yang Y.Q. and Suo Y.H., 2014. Geophysical interpretation and formation mechanism of the Yandang Low Uplift in the East China Sea Shelf Basin. *Chinese J. Geophys.*, **57**, 650-662.

Yang Q.L., 1992. Geotectonic framework of the East China Sea. In: Watkins J.S., Zhiqiang F. and McMillen K.J. (Eds), *Geology and Geophysics of Continental Margins*. American Association of Petroleum Geologists Memoir, **53**, 17–25.

Yang S., Hu S., Cai D., Feng X., Chen L. and Gao L., 2004. Present-day heat flow, thermal history and tectonic subsidence of the East China Sea Basin. *Mar. Petrol. Geol.*, **21**, 1095–1105.

Yang W.D., Cui Z.K. and Zhang Y.B., 2010. *Geology and Mineral Resources of the East China Sea*. Marine Press, Beijing, China (in Chinese).

Ye J., Qing H., Bend S.L. and Gu H., 2007. Petroleum systems in the offshore Xihu Basin on the continental shelf of the East China Sea. *AAPG Bull.*, **91**, 1167–1188.

Zhang H.T., 2001. Historical significances of the new round surveys for the land and resources. *Chinese Geol.*, **28(1)**, 4–8 (in Chinese).

Zhang M.H., 2011. *Gravity, Magnetic and Electric Data Processing and Interpretation Software RGIS*. Geological Press, Beijing, China (in Chinese).

Zhao J.H., 2004. The forming factors and evolution of the Mesozoic and Cenozoic basin in the East China Sea. *Offshore Oil*, **24**, 6–14 (in Chinese).

Zhong Q., Meng X.H. and Liu S.Y., 2007. Study on the geological body's edge detection of using gravity data. *Computing Techniques for Geophysical and Geochemical Exploration*, **29 (Suppl.)**, 35–38 (in Chinese).

Zhou J.J., Lin C.S. and Huan Y.C., 2013. Decreasing noise in magnetic anomaly detection basing on wavelet denoising. *Appl. Mech. Mater.*, **368–370**, 1860–1863.

Zhou Z., Zhao J. and Yin P., 1989. Characteristics and tectonic evolution of East China Sea. In: Zhu X. (Ed.), *Chinese Sedimentary Basins. Sedimentary Basins of the World 1*. Elsevier, Amsterdam, The Netherlands, 165–179.

Zhou Z.Y., Jianyi J., Zongting L., Fengli Y. and Keyun S., 2001. Basin inversion in Xihu Depression, East China Sea. *Gondwana Res.*, **4**, 844–845.